Desalination and Water Treatment
www.deswater.com

doi:10.5004/dwt.2018.22193

111 (2018) 351–360
April

Modifying *Amygdalus scoparia* biochar with MgO for eliminating tetracycline from aqueous solutions

Saeed Ardashiri, Seyedenayat Hashemi*†, Bahman Ramavandi, Sina Dobaradaran

Environmental Health Engineering Department, Faculty of Health, Bushehr University of Medical Sciences, Bushehr, Iran, Tel. +989382229579, email: mr.saeed2008@yahoo.com (S. Ardashiri), Tel. +989363311903, email: ramavandi_b@yahoo.com (B. Ramavandi), Tel. +989173731242, email: sina_dobaradaran@yahoo.com (S. Dobaradaran)
†Environmental Health Engineering Department, Faculty of Health and Nutrition, Bushehr University of Medical Sciences, Sabzabad Bolvd., 7518759577 Bushehr, Iran, Tel. +989177755384, Fax +987733450134, email: seyedenayat_hashemi@yahoo.com (S. Hashemi)

Received 2 October 2017; Accepted 16 March 2018

ABSTRACT

In this study, a biochar was provided from the wasted wood of *Amygdalus scoparia* tree and then modified with MgO to produce a biochar-MgO composite. This composite was then applied to remove tetracycline from aqueous solutions. The characteristics of the as-prepared composite were determined using X-ray diffraction, scanning electron microscopy, Fourier transform infrared spectroscopy, and specific surface area analysis. The specific surface area and pore volume of the adsorbent were obtained as 461 m^2/g and 0.2403 cm^3/g, respectively. The response surface method (RSM) based on central composite design (CCD) was successfully used for modeling and optimizing the tetracycline removal by the adsorbent. The effect of six independent variables including pH, tetracycline concentration, adsorbent dose, shaking rate, temperature, and contact time was explored on the tetracycline adsorption. The analysis of variance (ANOVA) of the quadratic model suggested that the predicted values were in good agreement with experimental data. Based on the RSM model, the maximum removal was obtained at the conditions of pH = 4, adsorbent dose = 0.414 mg/L, tetracycline concentration = 91 mg/L, contact time = 118 min, temperature = 49°C, and shaking rate = 63 rpm. The adsorption data well followed the Langmuir isotherm and the pseudo-second order kinetic model. Finally, thermodynamic parameters determined that the adsorption process was spontaneous and exothermic in nature.

Keywords: *Amygdalus scoparia*; Adsorption; Tetracycline removal; Biochar-MgO composite; Response surface methodology

1. Introduction

Pharmaceutical compounds are considered as emerging contaminants, which are mainly released from untreated waste waters of hospitals and pharmaceutical factories to the environment [1]. Due to the huge utilization of pharmaceutical compounds over the past decade, scientific communities are searching for solutions to distinguish the effect of pharmaceutical concentrations in the environment and water bodies. Among pharmaceuticals, antibiotics are annually used in large quantities (nearly 100,000–200,000 ton) to inhibit and cure bacterial diseases in humans and animals such as cattle, swine, poultry, and fish [2]. According to literature [3], because of incomplete metabolization of antibiotics in humans and animals body, about 30–90% of used antibiotics are excreted into the environment via urine or feces. Specifically, tetracycline's (TCs) class of antibiotics, which include tetracycline (TC), tetracycline hydrochloride, oxytetracycline, and chlortetracycline are widely utilized in livestock industry and human therapy. Tetracycline mole-

*Corresponding author.

cule is forcefully polar and has three proton active groups: a dimethyl ammonium, a tricarbonylamide group, and a phenolic diketone [4]. Further, TC is considered as the second most generated and utilized antibiotic in the world.

However, the concentrations of TCs in the treated waste waters are generally low, but they can accumulate in the soil, sediments, and water bodies, and then alter the resistance of bacteria corresponded to natural decontamination [5]. Thus, strict control and elimination of TC_S has become a vital subject for the environment and global health. The treatment techniques for eliminating pharmaceuticals from waste waters are advanced treatments (membrane process and adsorption methods,) as well as advanced oxidation processes (Fenton oxidation, ozone/hydrogen peroxide treatment, photo catalysis, and electrochemical oxidation, ultrasound, etc) [6]. Among the processes, the adsorption technique is the most attractive process because it is simple-to-design, facile-to-operate, and inexpensive method [7]. So far, many adsorbents have been used for pharmaceutical removal like magnetic resin [8], alkali biochar [9], nitrifying granular [10], illite [11] marine sediments [12], palygorskite [13], etc. The activated carbon is the famous adsorbent, but it has many challenges like the cost of production and non-renewable origin [14]. The agricultural waste materials and trees' wood [14] are, however, renewable, widely available, cheap, and environmentally friendly materials [15]. Thus, they can be used as precursors of biochar [16]. Biochar is a black solid particle that contains fine carbon (about 70–80%), which can be achieved from slow or fast biomass pyrolysis in the absence of oxygen [17]. Several materials have been used for production of biochar such as cherry seed [18], beech and pinewoods [19], grape bagasse [20], pine bark [21], and *Conocarpus erectus* [22]. Different procedure and chemical agents (e.g., H_3PO_4, KOH, H_2O_2, $ZnCl_2$, HNO_3, H_2SO_4, HCl, NaOH, and MgO) have been applied for activation and thus efficient pollutant removal [23,24]. One of the most attractive chemicals for modifying the adsorbents is magnesium oxide (MgO), since it is stable, nontoxic, inexpensive, and eco- friendly [25–27]. According to author's knowledge, there is no published paper about the activation of *Amygdalus scoparia* biochar with MgO.

Thus, the aims of this work included 1) modifying the biochar obtained from *A. scoparia* tree (a self-growing tree in many parts of the world such as Zagros Mountains, Iran) with MgO; 2) determining the surface characteristics of the biochar modified by MgO (biochar-MgO composite); 3) optimizing the influential parameters on the TC adsorption using response surface methodology (RSM); 4) assessing the kinetics, equilibrium, and thermodynamic of the adsorption process.

2. Materials and methods

2.1. Chemicals

All chemicals utilized in this study including tetracycline (purity > 98%), HNO_3 65%, NaOH, HCl, $Mg(NO_3)_2{\cdot}6H_2O$) were purchased from Merck Co., Germany. The main physiochemical properties of the tetracycline are: chemical formula = $C_{22}H_{24}N_2O_8$, pk_{a1} = 3.32, pk_{a2} = 7.78, pk_{a3} = 9.58, solubility = 22000 g/L, and molecular weight = 444.43 g/mol [28]. Deionized water was used for synthesizing all working solutions. A 1000-mg/L stock solution of TC was prepared by dissolving 512.8 mg TC in 500 mL deionized water in an Erlenmeyer flask. The stock solution of TC was diluted successively to prepare the required concentrations, and was kept at 4°C in a dark place.

2.2. Preparation and modification of biochar-MgO

The wasted wood of *Amygdalus scoparia* tree was collected from Zagros Mountains around Shiraz city, Iran. First, the *A. scoparia* wood was cut into pieces of 1 cm. The wood pieces were then washed several times with double distilled water to remove dust and impurities and then oven-dried at 105°C for 2 h. Next, about 20 g of the dried wood was put in an electric furnace (Carbolite, England) in the absence of O_2 for 2 h at 150°C. After that, the burned wood was submerged in a 250-mL HNO_3 1 M solution for 24 h in a shaker incubator (Parsazma, Iran) at 180 rpm. Then, the biochar was rinsed with deionized water until the pH of the elution liquid was brought to around 7. Thereafter, the wet biochar was put in the electric furnace in the absence of O_2 for 2 h at 400°C.

After preparing the HNO_3-treated biochar, the biochar-MgO composite was synthesized by sol-gel method. To do this, 20 g of biochar was added to 100 mL of $Mg(NO_3)_2{\cdot}6H_2O$ solution, and then 50 mL of NaOH 1 M solution was added in a drop-wise mode during 12 h to the solution. The solution was magnetically stirred (100 rpm) at the room temperature. The mixture was passed through Whatman filter No. 42 to obtain a gelatinous material. The obtained gel was washed several times with double distilled water and dried at 80°C for 24 h. The dried material was finally calcinated in the electric furnace at 450°C for 2 h to obtain biochar-MgO composite [29]. The biochar-MgO particles were finally sieved by ASTM (mesh no. 120) to achieve uniformed size material.

2.3. Measurements of surface characteristics

A pH meter (AS-3C Model, Shanghai Precision Scientific Instrument Co., China) was used for measuring the solution pH. The functional groups of biochar-MgO composite were detected by Fourier transform infrared spectroscopy (Bruker, Germany). Scanning electron microscopy (SEM) images were obtained by a JSM7500F at 3 kV and N_2 adsorption–desorption was conducted at –196°C using Brunauer–Emmett–Teller (BET) surface area apparatus (Micromeritics ASAP2020). Qualitative and quantitative analysis of chemical contents of the adsorbent was performed by an X-ray fluorescence analysis (XRF, X pert pro, Panolytical Co.).

The zeta potential charge was determined using zero point charge (pH_{ZPC}) measurement. To do this, initial pH values (pH_i) of 25 mL of NaCl 0.1 M solutions were adjusted within a pH range of 1–12 using HCl or NaOH 0.01–0.1 M. Then, 0.2 g biochar-MgO composite was added to the prepared solutions. The solutions were stirred for 24 h and then filtered. The final pH of the filtrate (pH_f) was also determined. The value of pH_{ZPC} of the biochar-MgO composite was obtained from the intersection of the curve of pHi *vs.* $\Delta pH_{i\text{-}f}$ [30].

2.4. Experimental design

RSM is a statistical and mathematical tool used to select the best experimental conditions with the lowest number of experiments. RSM designs include three-level factorial design such as central composite design (CCD), Box–Behnken design (BBD), and D-optimal design. The CCD statistic model, one of the most efficient and commonly used RSM models, is utilized to optimize the influence of independent variables on the response [31,32]**.** The ranges of the variables employed were selected based on the preliminary experiments as well as results in the literature. For a two-level study, the CCD consists of three operations namely: 2^k factorial runs, 2k axial runs, and k_c center runs. For six independent variables, the design involved 64 factorial points, 12 axial runs, and 10 replicates at the center points utilized for the purpose of estimating experimental error and the reproducibility of data. In this study, the independent variables were optimized for the removal efficiency of tetracycline. The ranges of independent variables and their coded levels are given in Table 1 [33,34].

All 86 experiments were calculated in a random order to minimize systematic errors. Each independent variable (X_i) was converted to coded values, according to Eq. (1).

$$X_i = \frac{X_i - X_i 0}{\Delta X_i} \tag{1}$$

where X_i is a dimensionless codified value of the factor, X_0 is the central value of the factor and ΔX refers to the difference between the high and central values of the factor.

The results of all CCD experimental runs were analyzed by the least-squares regression method to predict the process response and to estimate the coefficients according to the following second-order equation.

$$Y = \beta 0 + \sum_{(i=1)}^{k} \beta x_i + \sum_{i=1}^{k} \beta_{iix_i^2} + \sum_{i=1}^{k-1} \sum_{i=2}^{k} \beta_{ij} x_i x_j + \cdots + e \tag{2}$$

where Y refers to the response predicted by the model (TC removal efficiency), β_0 is the model constant (intercept term), X_i and X_j are the coded values of independent variables, β_i, β_{ii}, and β_{ij} are the linear, quadratic, and interaction coefficients, respectively, k is the number of factors studied and optimized, and e is the experimental error.

The polynomial model was obtained by multiple regression analysis. The estimated model equation was validated via the analysis of variance (ANOVA). The statistical significance of the model and terms was evaluated using P-value < 0.05 at a 95% confidence level. The validity and quality of the fit were expressed by the correlation coefficient (R^2). Therefore, the optimal values of six variables could be obtained by RSM.

Table 1
Independent variables and their coded levels based on central composite design

Parameters	Unit	Coded value				
		–2	–1	0	+1	+2
pH (A)	–	2	4	6	8	10
Initial conc. (B)	mg/L	50	60	70	80	100
Adsorbent dosage (C)	g	0.5	0.6	0.7	0.8	1
Agitating rotor (D)	rpm	50	70	90	110	120
Contact time (E)	min	30	60	90	120	180
Temperature (F)	°C	20	30	40	50	60

The TC concentration was determined by a UV–vis spectrophotometer (UV2550, Shimadzu, Japan) with wavelength of 357 nm [35]. The TC removal percentage (R%) and the amount of the TC adsorbed per gram of the biochar-MgO composite (q_t, mg/g) were evaluated using Eq. (3) and (4), respectively.

$$R\% = \left[\frac{C_0 - C_1}{C_0}\right] \times 100 \tag{3}$$

$$q_t = \left[\frac{C_0 - C_t}{M}\right] \times V \tag{4}$$

where C_0, C_1 and C_t are the initial, final, and the concentrations of TC at any time in the solution (mg/L), V is the volume of solution (L), and M is the weight of biochar-MgO composite (g).

2.5. Adsorption isotherms

The equilibrium data were evaluated by four "two-parameter isotherms" models including Langmuir, Freundlich, Dubinin–Radushkevich (D–R), and Temkin [36].

$$\frac{C_e}{q_e} = \frac{1}{q_{max} \times b} + \frac{C_e}{q_{max}} \tag{5}$$

$$R_L = \frac{1}{1 + bC_0} \tag{6}$$

$$\log q_e = \log k_f + \frac{1}{n} \log C_e \tag{7}$$

$$q_e = \ln q_{m-} k\varepsilon^2 \tag{8}$$

$$E_a = \frac{1}{\sqrt{2KD}} \tag{9}$$

$$q_{e\ =} q_m \ln \left(K_T C_e\right) \tag{10}$$

where C_e is the equilibrium concentration of TC (mg/L), q_e is the amount of TC antibiotic adsorbed by biochar-MgO composite at equilibrium, q_{max} (mg/g) and b are the Langmuir constants related to the adsorption capacity and energy, respectively. The separation factor (R_L) which has been utilized to assess the quality of the adsorption process (favorable: $0 < R_L < 1$, unfavorable: $R_L > 1$, or irreversible: $R_L = 0$). K_F (L/g) is Freundlich constant related to adsorption capacity and the n parameter denotes the adsorption intensity which has been utilized to evaluate when the adsorption process is physical ($n > 1$), chemical ($n < 1$), or linear ($n = 1$). q_m is the theoretical saturation capacity (mg/g), while k and ε are the constants related to the mean free energy of adsorption and Polanyi potential. The D–R constant can

give the mean energy of adsorption (E) by Eq. (9). The E parameter can be informative for revealing the type of adsorption mechanism (physical adsorption: E <8 KJ/mol, ion exchange: 8 < E <16 KJ/mol, and chemical adsorption: E > 16 KJ/mol) [37].

Temkin isotherm [Eq. (10)] represents the information about the heat of adsorption process and the strength of the bands formed between adsorbent and adsorbate.

2.6. Kinetic and thermodynamic parameter

The pseudo-first-order and pseudo-second-order model are applied for evaluating the kinetics of TC adsorption by biochar-MgO composite [38,39]:

$$log\left(q_e - q_t\right) = log\ q_e - \left(\frac{k1}{2.303}\right)t \tag{11}$$

$$\frac{t}{q_t} = \frac{1}{\left(k_2 \times q_e^{\ 2}\right)} + \left(\frac{1}{q_e}\right)t \tag{12}$$

where k_1 is the equilibrium rate constant of pseudo-first-order model (min^{-1}) and k_2 (g/mg min) represents the rate constant of the pseudo-second-order model.

The physical and chemical adsorption can be determined through thermodynamic parameters. The parameters of standard enthalpy (ΔH°, kJ/mol), standard entropy change (ΔS°, kJ/mol K), and standard Gibbs free energy change (ΔG°, kJ/mol) for the adsorption of TC onto biochar-MgO were calculated from the following equations [40]:

$$K_c = \frac{q_e}{c_e} \tag{13}$$

$$\Delta G° = -RT\ lnK_c \tag{14}$$

$$lnK_c = \frac{\Delta S}{R} - \frac{\Delta H°}{RT} \tag{15}$$

where K_c is the distribution coefficient, R is the universal gas constant (8.314 J/mol K), and T is the temperature (K).

3. Results and discussion

3.1. Adsorbent characteristics

The determination of the surface area of biochar is fundamental, as it may forcefully affect the reactive behavior of adsorbents and adsorbate. Thus, after production the biochar-MgO, their physical properties such as porosity, total pore volume, surface area were determined by the BET and BJH methods (see to Table 2). According to Table 2, the specific surface area (461.00 m^2/g) and the pore volume of the biochar-MgO are relatively high compared with other adsorbents such as peanut hulls [41], hydro char [42], and tomato waste [43]. Based on the BET equation, the pore diameter shows that the adsorbent is mesoporous. However, according to the BJH equation, the adsorbent is macroporous. Also, Fig. 1 shows the N_2 adsorption-desorption isotherm

Table 2
Surface characteristic of biochar-MgO

Characteristic	Value
Surface area	
Single point surface area at p/p° = 0.2	478.39 m^2/g
BET surface area	461.00 m^2/g
Langmuir surface area	609.33 m^2/g
t-Plot micropore area	397.25 m^2/g
t-Plot external surface area	63.74 m^2/g
Pore volume	
Single point adsorption total pore volume of pores less than 801.322 Å diameter at p/p° = 0.97	0.2403 cm^3/g
t-Plot micro pore volume	0.1846 cm^3/g
BJH Adsorption cumulative volume of pores between 17 Å and 3000 Å diameter	0.0606 cm^3/g
BJH adsorption cumulative volume of pores between 10 Å and 3000 Å width	0.0600 cm^3/g
Pore size	
Adsorption average pore width (4V/A by BET)	20.8545 Å
BJH Adsorption average pore diameter (4V/A)	65.51 Å
BJH desorption average pore diameter (4V/A)	60.61 Å

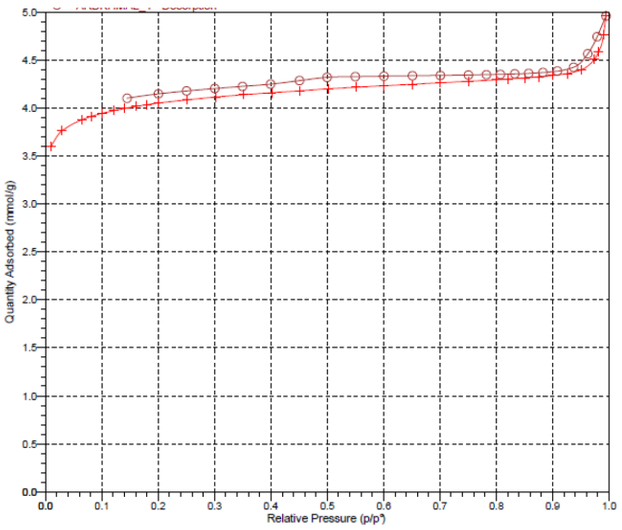

Fig. 1. Nitrogen adsorption/desorption isotherm (BET) of biochar-MgO composite.

of the biochar-MgO. Based on this figure, the adsorbent is classified as a type IV according to the International Union of Pure and Applied Chemistry [44,45]. In addition, the surface area of the biochar (without MgO modification) was found to be (305.07 m^2/g), which is much far than that of biochar-MgO. Therefore, rise of specific surface area of the biochar after modification with MgO is probably the main reason for tetracycline's proper adsorption in this work. In other studies [46,47], magnesium oxide has increased the surface area of adsorbents and, as a result, it increased the adsorption efficiency of the pollutants.

The SEM image was used to study the textural morphology and pore structure of the biochar-MgO composite. The SEM images of the adsorbent are depicted in Fig. 2. This figure shows that there are some nano-scale particles on the biochar surface, suggesting successful modification of crude adsorbent with magnesium oxide. Fig. 2b demonstrates that the biochar-MgO surface has a small amount of fine particles which may have been caused by the reaction of adsorbent and TC pollutant.

The FTIR spectra of fresh and used biochar-MgO composite are illustrated in Fig. 3. A sharp peak around 3907 cm^{-1}, can typically be attributed to the –OH stretching band in the $Mg(OH)_2$ crystal structure. It indicates that MgO might have reacted with the water vapor and formed $Mg(OH)_2$. The sharp peak at ~3437 cm^{-1} could be attributed to the –OH stretching vibration. The peak determined at ~2928 cm^{-1} can be assigned to the -CH_2 group bound. This peak shifted to 2930 cm^{-1} after the reaction, suggesting that the –CH_2 group was involved in TC binding. The sharp bands around 1430 cm^{-1} and 1725 are related to C=C and C=O stretching vibrations in carboxyl and alkenes, respectively. The C-CH and C-N stretching appeared at 1259 cm^{-1}, with band at ~598 cm^{-1} being related to the Mg-O stretching vibration [25,48].

To identify the purity and crystallinity of the biochar-MgO composite, XRD test was conducted (see Fig. 4). A peak at 2θ of 26° indicates the presence of large amounts of amorphous carbon particles or non-crystalline solid. In addition, the surface elemental compositions of the biochar-MgO were measured based on XRF test, with the results displayed in Table 3. The results show that the magnesium oxide is present in the adsorbent composition. as Also, the amount of magnesium oxide decreased after tetracycline absorption. The pH_{ZPC} (zeta potential) of the composite was obtained as 8.5. This means that at solution pH above and below 8.5, the adsorbent surface has a positive and negative charge, respectively.

In general, surface studies suggest that the mechanism of adsorption of tetracycline can depend on the following factors: 1) structural properties of tetracycline; 2) physiochemical properties of the adsorbent surface like pore size distribution, surface functionality, and specific surface area; and 3) solution pH [49].

3.2. RSM and 3D plots

The experimental data were detected and the response functions for TC removal efficiency were expressed using the second order equation model. Some terms in this model were not significant at the 95% confidence level. These insignificant terms were removed from the model for better estimation. The final coded model was extracted from CCD as Eq. (16).

$$\begin{aligned} Y = {} & +81.62 - 10.58\,A + 3.82B + 2.04C + .79D + .94E \\ & +1.95F + 2.03AB - .16AC - .19AD - 66AE - 56AF \\ & +22BC + .000BD + .094BE - .25BF + .062CD + \\ & .22CE - .13CF + .5DE - .094DF - 2.42A^2 - \\ & 1.6B^2 - 1.8C - 1.4D^2 - .58E^2 + .24F^2 \end{aligned} \quad (16)$$

where Y is the response variable (TC removal); A, B, C, D, E, F are independent variables of pH, TC concentration (mg/L), adsorbent dosage (mg/L), shaking rate (rpm), temperature (°C), and time (min), respectively.

The analysis of variance (ANOVA) and optimization of parameters are shown in Table 4. The value of Fisher's F-value is equal to 37.74. The large F value shows that the maximum variation in the percentage removal is explained by the model. The p-value also represents whether F-value is large enough to indicate significance of the parameters. Thus, a factor with p-value of less than 0.05 and large F-value is considered to be significant [31]. At optimum

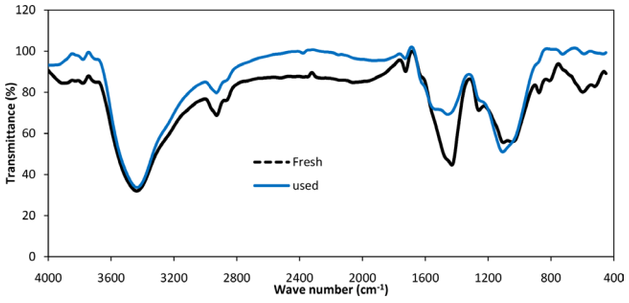

Fig. 3. FTIR spectra of fresh and used biochar-MgO composite.

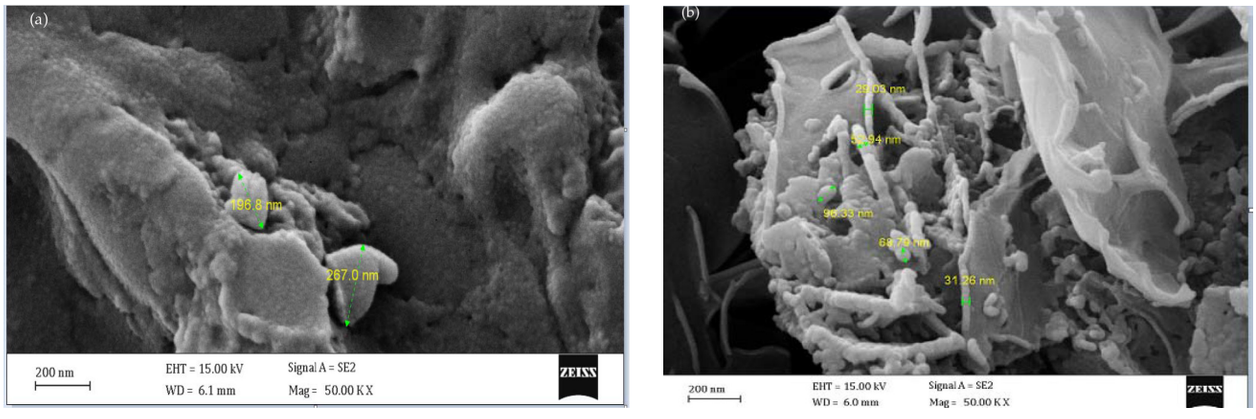

Fig. 2. SEM images of biochar -MgO composite (a) before and (b) after TC adsorption.

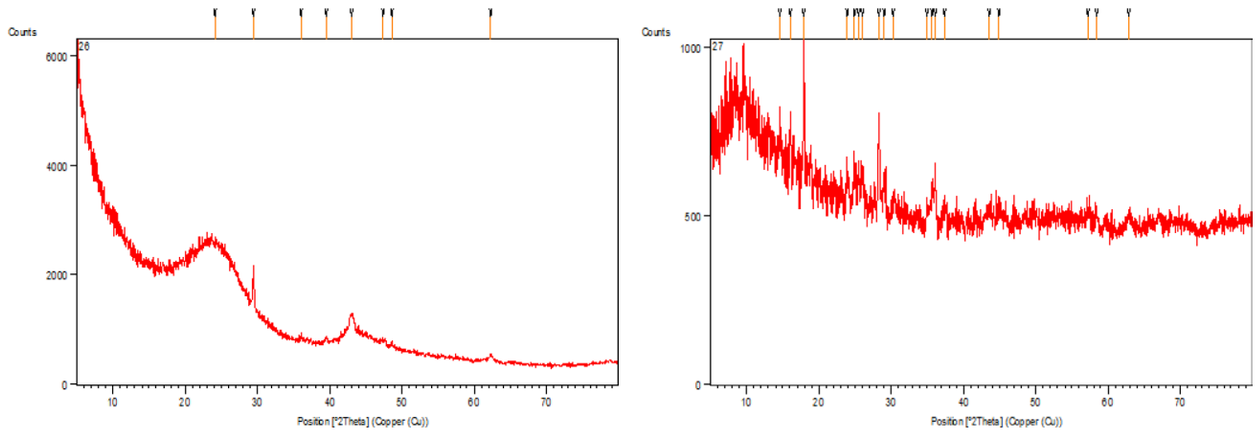

(a) (b)

Fig. 4. XRF pattern of biochar– MgO composite (a) before and (b) after TC adsorption.

Table 3
Elemental composition of biochar-MgO

Biochar-MgO	ZnO	Cl	Fe_2O_3	CaO	SO_3	P_2O_5	Al_2O_3	SO_3	SiO_2	MgO(%)
	(ppm)	(%)	(ppm)	(%)	(%)	(%)	(%)	(%)	(%)	(%)
Fresh	500	0.14	500	3.66	0.282	0.50	0.11	0.44	0.18	1.64
Used	–	–	450	3.04	23.938	0.40	–	2.44	0.11	0.28

Table 4
ANOVA results for the removal of TC by biochar-MgO composite

Source	Sum of Squares	Degree of freedom (df)	Mean square	F -value	P- value
Model	10427.64	27	386.21	37.74	<0.0001
A- pH	7706.64	1	7706.82	753.06	<0.0001
B-Concentration	1006.82	1	1006.82	98.32	<0.0001
C- Dosage (mg/L)	288.01	1	288.01	28.14	<0.0001
D- Shaking rate (rpm)	42.87	1	42.87	4.19	0.0452
E- Temperature (°C)	64.06	1	64.06	6.26	0.0152
F- Time (min)	261.96	1	261.96	25.60	0.00001

conditions (pH: 4, dosage: 0.414 g/L, shaking rate: 63 rpm, contact time: 118 min, temperature solution: 49°C), the estimated TC removal was obtained as 90.25%. The verification test was performed at the optimum conditions to check the validity of the proposed model. The experimental value of the TC removal under optimum conditions was obtained as 92.75%. Also, the adequate precision (equal to 22.072 > 4) indicates an adequate signal for the quadratic model and therefore, the model can be utilized to navigate the design space. In addition, a coefficient of variance (CV) of 4.23% (<10%) indicates the high accuracy and reliability of the experiment.

The significance of factors and their interactions are expressed by p-values. If the p-values Prop> F is <0.05 (95% confidence level), the model terms are significant. Also, the suitability and validity of the quadratic model was calculated by coefficient of determination (R^2). The value of R^2 and adjusted R^2 for the reduced model was obtained as 0.9461 and 0.9211, respectively, suggesting a satisfactory agreement between them. The adjusted R^2 was close enough to the R^2 value of 0.9461, revealing that the unnecessary factors have not been included in the model [50]. The R^2 value of 0.9461 indicates that 94.61% of variations occur in the TC removal efficiency explained by the independent variables and their interactions.

In order to illustrate the relationship between variables (pH, temperature, initial concentration, shaking rate, and adsorbent dose), the response surface graphs were plotted (see Fig. 5). The 3D response surface shown as graphical offering was applied to show the interactive effects of measurable variables on removal efficiency of TC. In this plot, the concurrent interaction of pH and initial TC con-

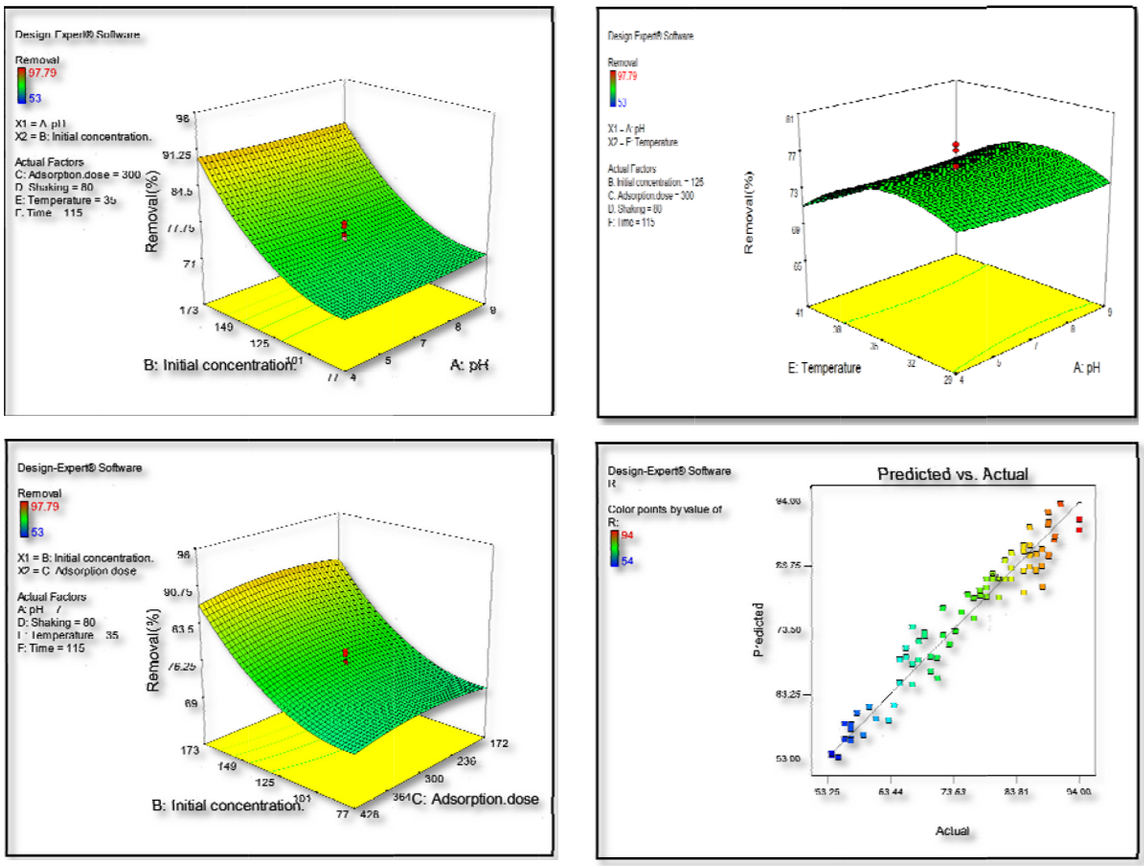

Fig. 5. 3D plot relation between pH, initial TC concentration, and removal efficiency and actual values versus predicted response by CCD.

centration on the removal of TC has been demonstrated in Fig. 5. Nevertheless, the other factors were kept constant at a central value encoded as value 0. As can be seen in Fig. 5, the removal efficiency of TC at pH 4 increased from 86% to 90% by elevating the concentration of TC from 77 mg/L to 173 mg/L. Also, by increasing the initial concentration of TC and increasing solution pH from 4 to 9, the TC removal efficiency grew from ~61% to ~73%. A further increase in the TC concentration and pH had a negative effect on adsorption process performance and subsequently decreased the TC removal efficiency. These results indicate that the solution pH can significantly affect the adsorption process and the TC removal was favorable in the weak acidic environment. High adsorption efficiencies were achieved at pH 4 (between $pK_{a,1}$ and $pK_{a,2}$), indicating that $TC^{(\pm 0)}$ has easily been adsorbed onto the biochar-MgO composite. It seems that $TC^{(\pm 0)}$ is adsorbed on the biochar–MgO through multiple interactions including hydrophobicity and surface complexes. At pHs higher than 7.68 (pK_{a2}), TC^{0-} was the major TC species. It can be hypothesized that the decrease of removal efficiency at pH 9 has mainly been due to the electrostatic repulsion and the weakening of hydrophobic function [51]. The removal of TC happened immediately at the beginning of the reaction, because of the abundant reactive sites available on the surface of fresh adsorbent. After 115 min, the adsorption occurred in a slow mode. Thus, the removal rate was restricted by the lack of reactive sorption sites [52]. Also, the decrease in removal efficiency may have been caused by the saturation of the limited number of active sites. Another cause can be the certain concentration at which the active sites become saturated.

3D plot relation between pH, temperature, and removal efficiency has been illustrated in Fig. 5. The high temperatures have an inverse effect on the removal efficiency, probably due to the release of the adsorbed TC into the solution, the degradation or deactivation of active sites on the adsorbent surface due to the breaking of the chemical bands, and the weakening of the force between the pollutant and active sites [53].

The effects of adsorbent dose and initial TC concentration on removal efficiency of TC are revealed in Fig. 5. By increasing the initial concentration of TC from 77 mg/L (at adsorbent dos of 0.172 g/L) to 173 mg/L (at adsorbent dose of 0.428 g/L), the removal efficiency rose from 72% to 85%. The positive relationship between the adsorbent dose and TC removal efficiency can be attributed to improved adsorbent specific surface area and availability of more adsorption sites. Nevertheless, with an increase in the initial TC concentration, the adsorption capacity

at equilibrium was enhanced. This is owing to raised concentration gradient, which acts as a driving force to prevail the persistence to mass transfer of tetracycline between the aqueous phase and biochar-MgO composite. Therefore, the maximum adsorption was achieved when 91 mg/L of initial TC concentration was used. Furthermore, Fig. 5 demonstrates the actual values versus predicted response of the empirical model. The results obtained from operating variables well agreed with the predicted data of the response from the empirical model. The model predicted the optimal values of the variables consisting of pH: 4, adsorbent dosage: 0.414 g/L, shaking rate: 63 rpm, contact time: 118 min, and temperature solution: 49°C.

3.3. Adsorption isotherm

Adsorption isotherm study is applied to determine the amounts of adsorbate removed from a solution at the equilibrium conditions by unit of adsorbent mass at a constant temperature. The results of four most common models (Langmuir, Freundlich, Temkin, and D–R) are provided in Table 5. Adsorption of TC onto biochar–MgO well fitted the Langmuir isotherm ($R^2 > 0.99$). The separation factor (R_L) value was obtained as 0.82. Thus, the adsorption process of TC onto the biochar-MgO composite is favorable within the studied concentration range. The maximum adsorption capacity was attained to be 111.1 mg/g, which is higher than that obtained for other adsorbents like peanut hulls [41] and hydro char [42], but smaller for tomato waste [43] and tyre char [42].

3.4. Adsorption kinetic

In order to study the kinetics of TC adsorption using biochar–MgO and to better identify the sorption process, pseudo-first order and pseudo-second order models were applied. The obtained kinetics parameters are listed in Table 6. Comparing the correlation coefficients of two kinetic models, it is clear that the pseudo-second order kinetic model fitted the adsorption data better. Further, Table 6 shows that according to most recent studies, the adsorption of tetracycline has followed pseudo-second order kinetics.

3.5. Adsorption thermodynamic

The effect of temperature on the adsorption of TC by biochar–MgO composite was calculated in batch experiments at solution temperatures of 298, 303, 313, 323, 328, and 333 K. The values of thermodynamic parameters are presented in Table 7. Based on data presented in Table 7, the negative values of ΔH^o indicate that the adsorption process is exothermic. This may be due to the total energy absorbed in bond breakdown is lower than the total energy released in bond development between TC and biochar–MgO composite, thus causing the release of extra energy in the form of heat to the solution [59]. The Gibbs energy change is a key factor for determining the degree of spontaneity of the adsorption process. A higher negative value of ΔG^o indicates that spontaneous physisorption has taken place in the system [59]. Also, the positive value of ΔS^o indicates that the adsorption process has involved a dissociative mechanism [59].

Table 7
Adsorption thermodynamic parameters

ΔH^o (kJ/mol)	ΔS^o (J/K mol)	ΔG^o (kJ/mol)			Adsorption nature
		303 K	313 K	323 K	
–4910.7	16.69	–3374	–4206	–4983	Exothermic

Table 5
Isotherms findings

Langmuir				Freundlich			Temkin			Dubinin–Radushkevich			
($y = 0.0091x + 0.0023$)				($y = -0.1937x + 3.2621$)			($y = -2.8466x + 24.951$)			($y = 8E\text{-}07x + 2.4946$)			
q_{max}	K_L	R_L	R^2	k_f	n	R^2	q_m	b_T	R^2	q_m	K_D	E_a	R^2
111.1	3.95	0.82	0.9924	2.46	5.2	0.9032	2. 84	1.0002	0.9116	15.06	21.67	0.15	0.7356

Table 6
Adsorption kinetic parameters and the comparison with different absorbent

Precursor	Activator	Adsorbate	C_o (mg/L)	Pseudo-first order		Pseudo- second order		Ref.
				R^2	k_1 (min^{-1})	R^2	k_2 (g/mg min)	
Macad shells	NaOH	TC	500	0.87	0.1286	0.95	4.7×10^{-4}	[54]
Vine wood	NaOH	TC	20	0.91	0.002	0.99	0.233	[55]
Petroleum coke	KOH	TC	100	0.886	4.5 E-2	0.959	7.2E-5	[56]
Activated carbon	$MnFe_2O_4$	TC	–	0.854	1.33	0.929	0.0049	[57]
Pumice stone	–	TC	5–300	0.998	0.03	0.999	0.02	[58]
Biochar	MgO	TC	91	0.986	–81.4	0.9979	0.003	This work

4. Conclusions

In this paper, the *Amygdalus scoparia* biochar was modified with MgO to remove tetracycline from aqueous media. The adsorbent was a non-crystalline solid and had a surface area of 461 m²/g. The response surface methodology (RSM) was used to optimize the influential parameters affecting the tetracycline adsorption. The maximum adsorption efficiency of TC (92.75%) was obtained at the optimized conditions of pH: 4, adsorbent dosage: 0.414 g/L, shaking rate: 63 rpm, contact time: 118 min, temperature solution: 49°C. Tetracycline adsorption data well fitted the Langmuir isotherm model (q_{max} = 111.1 mg/g) and the second-order kinetics. Also, thermodynamic parameters indicated that the process was spontaneous and exothermic. Generally, the biochar-MgO composite is an efficient adsorbent and has a suitable potential to be used in full-scale tetracycline treatment.

Acknowledgment

This paper was extracted from MSc. thesis of the first author. The authors would like to thank Bushehr University of Medical Sciences, Bushehr, Iran for providing financial support (Grant number: BPUMS- 95H-329) to conduct this research.

References

[1] R. Kafaei, F. Papari, M. Seyedabadi, S. Sahebi, R. Tahmasebi, M. Ahmadi, G.A. Sorial, G. Asgari, B. Ramavandi, Occurrence, distribution, and potential sources of antibiotics pollution in the water-sediment of the northern coastline of the Persian Gulf, Iran, Sci. Tot. Environ., 627 (2018) 703–712.
[2] H. Arfaeinia, K. Sharafi, S.E. Hashemi, B. Ramavandi, Reductive degradation of ciprofloxacin in aqueous using nano scale zero valent iron modificated by Mg-aminoclay, Int. J. Pharm Technol., 8 (2016) 13125–13136.
[3] G.A. Sayğılı, H. Sayğılı, F. Koyuncu, F. Güzel, Development and physico chemical characterization of a new magnetic nano composite as an economic antibiotic remover, Process Saf. Environ. Prot., 94 (2015) 441–451.
[4] H. Arfaeinia, K. Sharafi, S. Banafshehafshan, S.E. Hashemi, Degradation and biodegradability enhancement of chloramphenicol and azithromycin in aqueous solution using heterogeneous catalytic ozonation in the presence of MGO nano crystalin comparison with single ozonation, Int. J. Pharm Technol., 8 (2016) 10931–10948.
[5] P. Mahamallik, S. Saha, A. Pal, Tetracycline degradation in aquatic environment by highly porous MnO_2 nano sheet assembly, Chem. Eng. J., 276 (2015) 155–165.
[6] M.J. Ahmed, Adsorption of quinolone, tetracycline, and penicillin antibiotics from aqueous solution using activated carbons: Review, Environ. Toxicol. Pharmacol., 50 (2017) 1–10.
[7] M. Fooladvand, B. Ramavandi, Adsorption potential of NH_4Br-soaked activated carbon for cyanide removal from wastewater, Indian J. Chem. Technol., 22 (2015) 183–193.
[8] Q. Zhou, Z. Li, C. Shuang, A. Li, M. Zhang, M. Wang, Efficient removal of tetracycline by reusable magnetic micro spheres with a high surface area, Chem. Eng. J., 210 (2012) 350–356.
[9] P. Liu, W.-J. Liu, H. Jiang, J.-J. Chen, W.-W. Li, H.-Q. Yu, Modification of bio-char derived from fast pyrolysis of biomass and its application in removal of tetracycline from aqueous solution, Biores. Technol., 121 (2012) 235–240.
[10] Y.-J. Shi, X.-H. Wang, Z. Qi, M.-H. Diao, M.-M. Gao, S.-F. Xing, S.-G. Wang, X.-C. Zhao, Sorption and biodegradation of tetracycline by nitrifying granules and the toxicity of tetracycline on granules, J. Hazard. Mater., 191 (2011) 103–109.
[11] P.-H. Chang, Z. Li, J.-S. Jean, W.-T. Jiang, C.-J. Wang, K.-H. Lin, Adsorption of tetracycline on 2: 1 layered non-swelling clay mineral illite, Appl. Clay Sci., 67 (2012) 158–163.
[12] X.-R. Xu, X.-Y. Li, Sorption and desorption of antibiotic tetracycline on marine sediments, Chemosphere, 78 (2010) 430–436.
[13] P.-H. Chang, Z. Li, T.-L. Yu, S. Munkhbayer, T.-H. Kuo, Y.-C. Hung, J.-S. Jean, K.-H. Lin, Sorptive removal of tetracycline from water by palygorskite, J. Hazard. Mater., 165 (2009) 148–155.
[14] R. Crisafully, M.A.L. Milhome, R.M. Cavalcante, E.R. Silveira, D. De Keukeleire, R.F. Nascimento, Removal of some polycyclic aromatic hydrocarbons from petrochemical wastewater using low-cost adsorbents of natural origin, Biores. Technol., 99 (2008) 4515–4519.
[15] M. Kılıç, Ç. Kırbıyık, Ö. Çepelioğullar, A.E. Pütün, Adsorption of heavy metal ions from aqueous solutions by bio-char, a by-product of pyrolysis, Appl. Surf. Sci., 283 (2013) 856–862.
[16] G. Li, B. Shen, F. Li, L. Tian, S. Singh, F. Wang, Elemental mercury removal using biochar pyrolyzed from municipal solid waste, Fuel Process Technol., 133 (2015) 43–50.
[17] A. Demirbas, Effects of temperature and particle size on biochar yield from pyrolysis of agricultural residues, J. Anal. Appl. Pyrol., 72 (2004) 243–248.
[18] G. Duman, C. Okutucu, S. Ucar, R. Stahl, J. Yanik, The slow and fast pyrolysis of cherry seed, Biores. Technol., 102 (2011) 1869–1878.
[19] E. Grieco, G. Baldi, Analysis and modelling of wood pyrolysis, Chem. Eng. Sci., 66 (2011) 650–660.
[20] İ. Demiral, E.A. Ayan, Pyrolysis of grape bagasse: Effect of pyrolysis conditions on the product yields and characterization of the liquid product, Biores. Technol., 102 (2011) 3946–3951.
[21] A. Güngör, S. Önenç, S. Uçar, J. Yanik, Comparison between the "one-step" and "two-step" catalytic pyrolysis of pine bark, J. Anal. Appl. Pyrol., 97 (2012) 39–48.
[22] F. Papari, P.R. Najafabadi, B. Ramavandi, Fluoride ion removal from aqueous solution, groundwater, and seawater by granular and powdered *Conocarpus erectus* biochar, Desal. Water Treat., 65 (2017) 375–386.
[23] M.C. Ncibi, R. Ranguin, M.J. Pintor, V. Jeanne-Rose, M. Sillanpää, S. Gaspard, Preparation and characterization of chemically activated carbons derived from Mediterranean *Posidonia oceanica* (L.) fibres, J. Anal. Appl. Pyrol., 109 (2014) 205–214.
[24] R. Azargohar, A.K. Dalai, Steam and KOH activation of biochar: Experimental and modeling studies, Micropor. Mesopor. Mater., 110 (2008) 413–421.
[25] E.M. Kalhori, T.J. Al-Musawi, E. Ghahramani, H. Kazemian, M. Zarrabi, Enhancement of the adsorption capacity of the light-weight expanded clay aggregate surface for the metronidazole antibiotic by coating with MgO nano particles: Studies on the kinetic, isotherm, and effects of environmental parameters, Chemosphere, 175 (2017) 8–20.
[26] B. Ramavandi, M. Jafarzadeh, S. Sahebi, Removal of phenol from hyper-saline wastewater using Cu/Mg/Al-chitosan-H_2O_2 in a fluidized catalytic bed reactor, React. Kinet. Mech. Catal., 111 (2014) 605–620.
[27] S.B. Mortazavi, B. Ramavandi, G. Moussavi, Chemical reduction kinetics of nitrate in aqueous solution by Mg/Cu bimetallic particles, Environ. Technol., 32 (2011) 251–260.
[28] Y.A. Ouaissa, M. Chabani, A. Amrane, A. Bensmaili, Removal of tetracycline by electro coagulation: Kinetic and isotherm modeling through adsorption, J. Environ. Chem. Eng., 2 (2014) 177–184.
[29] B. Ramavandi, A. Rahbar, S. Sahebi, Effective removal of Hg^{2+} from aqueous solutions and seawater by *Malva sylvestris*, Desal. Water Treat., 57 (2016) 23814–23826.
[30] F.S. Sarvestani, H. Esmaeili, B. Ramavandi, Modification of *Sargassum angustifolium* by molybdate during a facile cultivation for high-rate phosphate removal from wastewater: structural characterization and adsorptive behavior, 3 Biotech, 6 (2016) 251.
[31] M. Ravanipour, R. Kafaei, M. Keshtkar, S. Tajalli, N. Mirzaei, B. Ramavandi, Fluoride ion adsorption onto palm stone: Optimization through response surface methodology, isotherm, and adsorbent characteristics data, Data in Brief, 12 (2017) 471–479.

[32] D.R. Vakilabadi, B. Ramavandi, A.H. Hassani, G. Omrani, Optimization of metal component, characterization, and stability of Cu/Mg/Al–chitosan catalyst in catalytic ozonation of a landfill leachate, Desal. Water Treat., 80 (2017) 89–99.
[33] G. Asgari, B. Ramavandi, S. Farjadfard, Abatement of azo dye from wastewater using bimetal-chitosan, Scient. World J., 2013 (2013).
[34] G. Asgari, B. Ramavandi, S. Sahebi, Removal of a cationic dye from wastewater during purification by *Phoenix dactylifera*, Desal. Water Treat., 52 (2014) 7354–7365.
[35] H. Dong, Z. Jiang, C. Zhang, J. Deng, K. Hou, Y. Cheng, L. Zhang, G. Zeng, Removal of tetracycline by Fe/Ni bimetallic nano particles in aqueous solution, J. Colloid Interface Sci., 513 (2018) 117–125.
[36] Z. Li, L. Schulz, C. Ackley, N. Fenske, Adsorption of tetracycline on kaolinite with pH-dependent surface charges, J. Colloid Interface Sci., 351 (2010) 254–260.
[37] Z. Khademi, B. Ramavandi, M.T. Ghaneian, The behaviors and characteristics of a mesoporous activated carbon prepared from *Tamarix hispida* for Zn (II) adsorption from wastewater, J. Environ. Chem. Eng., 3 (2015) 2057–2067.
[38] M. Ahmadi, E. Kouhgardi, B. Ramavandi, Physico-chemical study of dew melon peel biochar for chromium attenuation from simulated and actual waste waters, Korean J. Chem. Eng., 33 (2016) 2589–2601.
[39] A. Ebrahimi, S. Hashemi, S. Akbarzadeh, B. Ramavandi, Modification of green algae harvested from the Persian Gulf by L-cysteine for enhancing copper adsorption from wastewater: Experimental data, Chem. Data Collect., 2 (2016) 36–42.
[40] R. Foroutan, F.S. Khoo, B. Ramavandi, S. Abbasi, Heavy metals removal from synthetic and shipyard wastewater using phoenix dactylifera activated carbon, Desal. Water Treat., 82 (2017) 146–156.
[41] J. Torres-Pérez, C. Gérente, Y. Andrès, Sustainable activated carbons from agricultural residues dedicated to antibiotic removal by adsorption, Chin. J. Chem. Eng., 20 (2012) 524–529.
[42] R. Acosta, V. Fierro, A.M. de Yuso, D. Nabarlatz, A. Celzard, Tetracycline adsorption onto activated carbons produced by KOH activation of tyre pyrolysis char, Chemosphere, 149 (2016) 168–176.
[43] H. Sayğılı, F. Güzel, Effective removal of tetracycline from aqueous solution using activated carbon prepared from tomato (*Lycopersicon esculentum* Mill.) industrial processing waste, Ecotoxicol. Environ. Saf., 131 (2016) 22–29.
[44] M.a.A. Aramendía, V. Borau, C. Jiménez, J.M. Marinas, J.R. Ruiz, F.J. Urbano, Influence of the preparation method on the structural and surface properties of various magnesium oxides and their catalytic activity in the Meerwein–Ponndorf–Verley reaction, Appl. Catal., A. 244 (2003) 207–215.
[45] N. Ranjbar, S. Hashemi, B. Ramavandi, M. Ravanipour, Chromium(VI) removal by bone char-ZnO composite: Parameters optimization by response surface methodology and modeling, Environ. Prog. Sustain. Energ., (2018) DOI: 10.1002/ep.12854. In Press.
[46] M. Hu, X. Yan, X. Hu, J. Zhang, R. Feng, M. Zhou, Ultra-high adsorption capacity of MgO/SiO_2 composites with rough surfaces for Congo red removal from water, J. Colloid Interface Sci., 510 (2018) 111–117.
[47] X. Zheng, M. Huang, Y. You, X. Fu, Y. Liu, J. Wen, One-pot synthesis of sandwich-like MgO@Carbon with enhanced sorption capacity of organic dye, Chem. Eng. J., 334 (2018) 1399–1409.
[48] S.K. Arfaeinia1H, S. Banafshehafshan, S. Hashemi, Degradation and biodegradability enhancement of chloramphenicol and azithromycin in aqueous solution using heterogeneous catalytic ozonation in the presence of MGO nano crystalin comparison with single ozonation, Int. J. Pharm. Technol., 8 (2016) 10931–10948.
[49] B. Ramavandi, G. Asgari, Comparative study of sun-dried and oven-dried Malva sylvestris biomass for high-rate Cu (II) removal from wastewater, Process Saf. Environ. Protect., 116 C (2018) 61–73.
[50] A.-A. Salarian, Z. Hami, N. Mirzaei, S.M. Mohseni, A. Asadi, H. Bahrami, M. Vosoughi, A. Alinejad, M.-R. Zare, N-doped TiO_2 nano sheets for photo catalytic degradation and mineralization of diazinon under simulated solar irradiation: Optimization and modeling using a response surface methodology, J. Mol. Liq., 220 (2016) 183–191.
[51] Ö. Hanay, B. Yıldız, S. Aslan, H. Hasar, Removal of tetracycline and oxytetracycline by micro scale zerovalent iron and formation of transformation products, Environ. Sci. Pollut. Res., 21 (2014) 3774–3782.
[52] H. Chen, H. Luo, Y. Lan, T. Dong, B. Hu, Y. Wang, Removal of tetracycline from aqueous solutions using polyvinylpyrrolidone (PVP-K30) modified nano scale zero valent iron, J. Hazard. Mater., 192 (2011) 44–53.
[53] A. Teimouri, H. Esmaeili, R. Foroutan, B. Ramavandi, Adsorptive performance of calcined Cardita bicolor for attenuating Hg (II) and As (III) from synthetic and real waste waters, Korean J. Chem. Eng., (2017) 1–10.
[54] A.C. Martins, O. Pezoti, A.L. Cazetta, K.C. Bedin, D.A. Yamazaki, G.F. Bandoch, T. Asefa, J.V. Visentainer, V.C. Almeida, Removal of tetracycline by NaOH-activated carbon produced from macadamia nut shells: Kinetic and equilibrium studies, Chem. Eng. J., 260 (2015) 291–299.
[55] H. Pouretedal, N. Sadegh, Effective removal of Amoxicillin, Cephalexin, Tetracycline and Penicillin G from aqueous solutions using activated carbon nano particles prepared from vine wood, J. Water Process Eng., 1 (2014) 64–73.
[56] D. Zhang, J. Yin, J. Zhao, H. Zhu, C. Wang, Adsorption and removal of tetracycline from water by petroleum coke-derived highly porous activated carbon, J. Environ. Chem. Eng., (2015).
[57] L. Shao, Z. Ren, G. Zhang, L. Chen, Facile synthesis, characterization of a Mn Fe_2O_4/activated carbon magnetic composite and its effectiveness in tetracycline removal, Mater. Chem. Phys., 135 (2012) 16–24.
[58] U.A. Guler, M. Sarioglu, Removal of tetracycline from waste water using pumice stone: equilibrium, kinetic and thermodynamic studies, Iranian J. Environ. Health Sci. Eng., 12 (2014) 79.
[59] H.N. Tran, S.-J. You, H.-P. Chao, Thermodynamic parameters of cadmium adsorption onto orange peel calculated from various methods: a comparison study, J. Environ. Chem. Eng., 4 (2016) 2671–2682.